A MODULAR PERCUSSION SYNTHESIS ENVIRONMENT

Stefan Bilbao[*]

Acoustics and Fluid Dynamics Group/Music,
University of Edinburgh
Edinburgh, UK
sbilbao@staffmail.ed.ac.uk

ABSTRACT

The construction of new virtual instruments is one long-term goal of physical modeling synthesis; a common strategy across various different physical modeling methodologies, including lumped network models, modal synthesis and scattering based methods, is to provide a canonical set of basic elements, and allow the user to build an instrument via certain specified connection rules. Such an environment may be described as modular.

Percussion instruments form a good test-bed for the development of modular synthesis techniques—the basic components are bars and plates, and may be accompanied by connection elements, with a nonlinear character. Modular synthesis has been approached using all of the techniques mentioned above, but time domain finite difference schemes are an alternative, allowing many problems inherent in the above methods, including computability, large memory and precomputation requirements, and lack of extensibility to more complex systems, to be circumvented.

One such network model is presented here along with the associated difference schemes, followed by a discussion of implementation details, the issues of excitation and output, and a description of various instrument configurations. The article concludes with a presentation of simulation results, generated in the Matlab prototyping language.

1. INTRODUCTION

Physical modeling sound synthesis has been applied, traditionally, for two distinct purposes: one is the emulation of existing musical instruments, but another is the creation of new musical instruments without an acoustic counterpart or reference, which retain the underpinnings of the laws of physics. If it is the second goal which is of interest, then a modular approach, employing well-understood canonical, or primitive elements is often taken, and the user (composer) is given the additional role of an instrument designer, and must necessarily specify connections among various instances of the primitive elements, in order to build an instrument. The hopes of such an approach are twofold: first, to obtain synthetic sound which possesses an acoustic character but which is, nevertheless, new, and second, to retain the ease of control and playability which is a great benefit of any physical modeling synthesis strategy.

Modularity has been approached in all physical modeling methodologies. The earliest and most profound influence is due to work on networks of mass-spring elements by Cadoz [1], which subsequently developed into the CORDIS and CORDIS ANIMA sound synthesis environments [2, 3, 4]. Modal synthesis [5, 6] and functional transformation approaches [7] also incorporate modularity as a fundamental feature, as do methods based on scattering networks employing components such as digital waveguides and wave digital filters [8, 9]. Beyond modularity, other issues of great relevance, at least to the programmer/algorithm designer, are the operation count, memory requirements, precomputation, and programming complexity [10].

There are advantages and disadvantages to all of the above methods. Lumped methods, which are based on primitive elements such as masses and springs, allow for quite flexible modular connection among elements, but the modeling of distributed elements, such as those that appear in acoustic musical instruments is awkward—certain components, such as stiff bars and plates may only be modeled in this way using very elaborate design procedures. Modal synthesis methods can produce solutions of extreme fidelity to an underlying model problem, but only provided that one has modal data available—in some cases this is easy to obtain, but in others, potentially large eigenvalue problems must be solved, before run-time, in order to obtain such data (an excellent example of such a system is a rectangular plate under free boundary conditions); memory requirements can be very large if the modal shapes or their values at a set of specified locations are stored, as they often are in implementation [11]. In addition, modal and functional transformation methods do not extend easily to incorporate nonlinearities of distributed type, though various techniques have been proposed [12, 13]. Scattering methods allow for extremely efficient solutions for distributed components which behave nearly according to the 1D wave equation (such as linear, non-stiff strings). But such an efficiency advantage does not extend to stiff or nonlinear systems, or to systems in 2D, such as plates and membranes. The modular connection among elements is usually carried using scattering operations, and, when lumped elements are modeled, using wave digital filtering blocks. While attractive in the linear case, when nonlinearities are present, such designs become problematic, leading to solutions requiring power-normalized waves (necessary for any nonlinear stability analysis) and iterative methods, and for which solutions may not be unique, and which may require a delicate ordering of operations in the run-time loop—indeed, it can be difficult to employ more than a single nonlinearity in a given network [14, 15].

Time domain finite difference schemes based on distributed canonical elements offer a means of sidestepping many of the above problems; precomputation and memory requirements are minimal, and there are not the usual data flow complexities which arise in scattering networks, even when many nonlinearities are simultaneously present. In addition, provable stability conditions are available, even under nonlinear conditions, based on energy analysis

[*] This work was supported by the Engineering and Physical Sciences Council UK, under grant number C007328/1.

[16]. In addition, such schemes, as they do not rely on particular assumptions such as the existence of a modal representation, or of traveling wave solutions, may be easily extended to handle distributed nonlinear models as well. On the other hand, the operation count may be larger than for some of the above methods, though normally not by much, except in the case of digital waveguides, in cases when they may be employed.

Percussion instruments form a very fertile test-bed for the development of such methods—excitation is relatively simple, compared to the case of, say, wind instruments and bowed string instruments, for which the model of the excitation element is crucial, and, furthermore, such instruments will produce musical sound under a wide variety of playing conditions, which may not be true in the case of the wind and bowed string instruments mentioned above. This is an especially important consideration if one is designing novel instrument without a real-world reference; the parameter space to be navigated by the eventual user may be large, and if the playability region is small, frustrations can arise!

A description of a modular percussion synthesis environment appears in Section 2, including PDE descriptions of the basic bar and plate elements (strings and membranes could equally well be treated, but because computational expense is relatively large for simulations of such components, they will not be discussed here), connecting elements which behave as nonlinear springs and dampers, excitation, and multichannel output. A simulation routine based on finite difference approximations appears in Section 3, accompanied by a discussion of stability conditions, computational complexity, and implementation issues. Simulation results are presented in Section 4, and sound examples are provided on the author's website, at

`http://ccrma.stanford.edu/~bilbao/soundex/bpnet/`

2. INSTRUMENT FORMULATION

In the context of percussion instruments, the main elements of interest will be bars, and plates. Simple linear models of both will be presented here, though in a finite difference framework, there is little difficulty in extending such models to include distributed nonlinear phenomena—see, e.g., [16]. In addition to these primitive distributed elements, a type of connection is necessary. Drawing inspiration from lumped network approaches, as well as similar instances of acoustic instruments involving such couplings, such as the prepared piano, a connection model behaving as a combination of a damper, a linear spring, and a cubic nonlinear spring will be presented here. See Figure 1, showing a representation of a general instrument configuration.

2.1. Bars

A simple model of linear uniform bar vibration is given by the following partial differential equation:

$$u_{tt} = -\frac{EI}{\rho A} u_{xxxx} - 2\sigma_0 u_t + 2\sigma_1 u_{txx} + \frac{1}{\rho A} \sum_q e_q f_q \quad (1)$$

Here, $u = u(x,t)$ is the transverse displacement of such a bar, depending on time $t \geq 0$ and a spatial coordinate $x \in [0, L]$, where L is the bar length. Sucbscripts t and x refer to temporal and spatial differentiation, respectively. The constants ρ, A, E and I are the mass density, cross-sectional area, Young's modulus and moment of inertia for the bar respectively; all are assumed constant here. The term with coefficient σ_0, on its own, gives rise

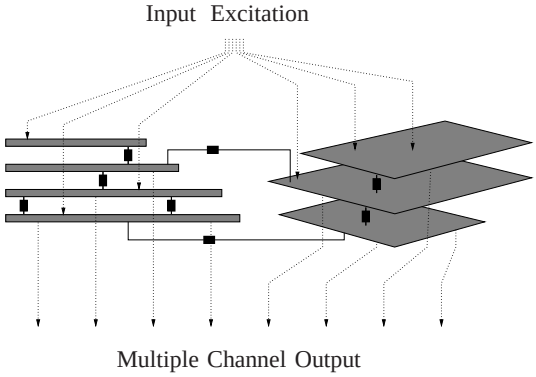

Figure 1: *A percussion synthesis network, composed of a set of bars (at left) and plates (at right); connections between elements at specified locations are indicated by dark lines and rectangles. Input consists of a series of pulses delivered to the network at specified locations, and multiple channel output is drawn from distinct locations in the network.*

to frequency-independent loss, and the term with coefficient σ_1 allows for increased loss at higher frequencies, which is characteristic of most percussion instruments. The final term involves a series of functions $f_q = f_q(t)$, with dimensions of force, representing either externally supplied excitations, or couplings to other objects—both such types of force will be described in subsequent sections. The distributions $e_q = e_q(x)$, which indicate the locations at which the excitations are to be applied are usually sharply peaked in a percussion setting, perhaps of the form of Dirac delta functions $e_q(x) = \delta(x - x_q)$ selecting a location $x = x_q$, but need not be.

This model may be extended to allow for a spatial dependence of the various parameters on x (giving models of, e.g., arched bars [17]), high-amplitude nonlinearity [18], more elaborate models of loss [19], and to include tensioning effects, in which case the model is better described as a stiff string [20]. For more on this model of bar vibration, and the various extensions mentioned above, see, e.g., [16].

In order to reduce the size of the parameter space faced by the eventual user, it is useful to introduce the scaling variable $x' = x/L$; upon the substitution of this variable, and after removal of primes, the resulting equation of motion is

$$u_{tt} = -\kappa^2 u_{xxxx} - 2\sigma_0 u_t + 2\sigma_1 u_{txx} + \sum_q E_q F_q \quad (2)$$

now defined over the unit interval $x \in [0, 1]$, and where here, $\kappa = \sqrt{EI/\rho A}/L^2$ is a stiffness parameter, which scales roughly with pitch, and where $F_q = f_q/M$ is an excitation function with dimensions of acceleration, where $M = \rho A L$ is the total mass of the bar; the scaled distribution E_q is defined as $E_q = L e_q$.

There are many possible boundary terminations for such a system at an endpoint at $x = 0$ or $x = 1$. Here are three of interest in a musical setting:

$$u = u_x = 0 \qquad \text{Clamped} \quad (3a)$$

$$u = u_{xx} = 0 \qquad \text{Pivoting} \quad (3b)$$

$$u_{xx} = \kappa^2 u_{xxx} - 2\sigma_1 u_{xt} = 0 \qquad \text{Free} \quad (3c)$$

All are lossless; many other terminations, involving masses, springs, and dampers, possibly nonlinear are possible, but this simple set will suffice for the present study.

A single bar is thus characterized by the three parameters κ, σ_0 and σ_1, as well as choices of possible boundary conditions at either end (nine, not counting multiplicities). κ, as mentioned above, scales roughly with pitch, but the placement of the resulting modal frequencies (nearly always inharmonic) is strongly dependent on the choice of boundary condition. σ_0 and σ_1 allow two-parameter control over damping rates. More useful perhaps to the musician is the 60 dB decay time, as a function of frequency f in Hz, which may be written [16] as

$$T_{60}(f) = \frac{6\ln(10)}{\sigma_0 + 2\pi\sigma_1 f/\kappa}$$

2.2. Plates

A simple model of the linear vibration of thin uniform plates is an extension of the above model to 2D:

$$u_{tt} = -\frac{D}{\rho H}\Delta\Delta u - 2\sigma_0 u_t + 2\sigma_1 \Delta u_t + \frac{1}{\rho H}\sum_q e_q f_q \quad (4)$$

Here, $u(x, y, t)$ represents transverse displacement of the plate, defined for time $t \geq 0$; in this article, for simplicity, the plate is assumed defined over the rectangular region $x \in [0, L_x]$, $y \in [0, L_y]$. The subscript t again represents partial time differentiation, and Δ is the Laplacian, which in Cartesian coordinates, is defined as

$$\Delta u = u_{xx} + u_{yy} \quad (5)$$

where subscripts x and y represent partial differentiation in the two spatial coordinates. ρ is the mass density, H the plate thickness, and the parameter D is defined as $D = EH^3/12(1-\nu^2)$, where E is Young's modulus, and ν is Poisson's ratio for the material. σ_0 and σ_1 are loss parameters, as in the case of the bar—they may be related to a frequency-dependent decay time in exactly the manner described at the end of the last section. As before, $f_q = f_q(t)$ represents a force due to external excitation or a coupling, applied at the spatial location described by a distribution $e_q = e_q(x, y)$.

Again, it is useful to simplify the system above by introducing the coordinates $x' = x/\sqrt{L_x L_y}$, $y' = y/\sqrt{L_x L_y}$—after subsitution in the system above, and removal of primes, the system becomes

$$u_{tt} = -\kappa^2 \Delta\Delta u - 2\sigma_0 u_t + 2\sigma_1 \Delta u_t + \sum_q E_q F_q \quad (6)$$

which is now defined over the unit area region $x \in [0, \alpha]$, $y \in [0, 1/\alpha]$, where $\alpha = \sqrt{L_x/L_y}$ is the plate aspect ratio. $\kappa = \sqrt{D/\rho H}/L_x L_y$ is again a stiffness parameter, scaling roughly with pitch, and where $F_q = f_q/M$ is defined in terms of the total plate mass $M = \rho H L_x L_y$, and $E_q = L e_q$.

Boundary conditions generalizing those of the bar may be written as

$$\begin{aligned} u &= u_n = 0 \qquad \text{Clamped} \\ u &= u_{nn} = 0 \qquad \text{Pivoting} \\ u_{nn} + \nu u_{ss} &= \kappa^2 \left(u_{nnn} + (2-\nu) u_{nss}\right) - 2\sigma_1 u_{nt} = 0 \qquad \text{Free} \end{aligned} \quad (7)$$

at an edge with normal coordinate n and tangential coordinate s [21]. (An extra corner condition, $u_{ns} = 0$, is necessary for two adjoining free edges.)

A given plate, then, is characterized by the five parameters κ, ν, α, σ_0 and σ_1, as well as choices of boundary condition at the four edges (there are then 81 possible configurations, again not counting multiplicities).

2.3. Connecting Elements

As an example of a single connection between two basic elements of bar or plate type, consider the following pair of PDEs:

$$\begin{aligned} u_{tt}^{(1)} &= \ldots + F_c E_c^{(1)} \\ u_{tt}^{(2)} &= \ldots + F_c^* E_c^{(2)} \end{aligned}$$

where $^{(1)}$ and $^{(2)}$ refer to the first and second element, respectively, and where the ... refer to the remaining terms in the PDEs, of the forms given in (2) and (6). The two elements are assumed to have masses $M^{(1)}$ and $M^{(2)}$, respectively.

F_c and F_c^* can be related in many ways—a simple general choice is of a nonlinear spring/damper connection, of the form

$$F_c = -\omega_0^2 \eta - \omega_1^4 \eta^3 - 2\sigma_\times \dot{\eta} \quad (8a)$$

$$F_c^* = -\mathcal{M}_{1/2} F_c \quad (8b)$$

where the term with coefficient ω_0 describes a linear spring connection, that with coefficient ω_1 a cubic nonlinear spring connection, and that with coefficient $2\sigma_\times$ a linear damping mechanism—the dot above η in this term signifies time differentiation. The constant $\mathcal{M}_{1/2} = M^{(1)}/M^{(2)}$ is the mass ratio of the two elements. The lumped quantity η is defined as

$$\eta = \langle u^{(1)}, E_c^{(1)} \rangle - \langle u^{(2)}, E_c^{(2)} \rangle \quad (9)$$

where $\langle \cdot, \cdot \rangle$ signifies an L_2 inner product over the appropriate space (1D in the case of a bar, and 2D in the case of the plate). Notice that if the distributions $E_c^{(1)}$ and $E_c^{(2)}$ are highly localized, then η reduces to a simple measure of the relative displacement of the two objects at the connection point.

Such a connection may be shown to be strictly dissipative (and lossless if $\sigma_\times = 0$).

2.4. Excitation

In a true model of synthesis based on a percussion instrument, a model of the excitation mechanism (a mallet or hammer) is necessary. In general, this interaction is nonlinear, and will depend strongly on the mass and stiffening characteristics of the mallet—see, e.g., [22] for the case of such a model as applied to a kettledrum. In the context of sound synthesis, rather than that of the pure investigation of musical instrument acoustics, one may note that the interaction time in most instruments is quite small (on the order of 1–5 ms), and thus as a shortcut, one may make use of a predefined form of the excitation function $F = F_e(t)$, in the case of both bars and plates. A simple pulse-like form, depending on few parameters, is the following raised cosine distribution:

$$F_e(t) = \begin{cases} \frac{F_{\max}}{2}\left(1 - \cos(\frac{2\pi(t-t_0)}{t_e})\right) & t_0 \leq t \leq t_0 + t_e \\ 0 & \text{otherwise} \end{cases} \quad (10)$$

Here, t_0 is the time at which the excitation occurs, t_e is its duration, and $F_{\max}$ is its maximum amplitude. Generally, under linear conditions, increases in $F_{\max}$ lead to an increase in output amplitude, while decreases in t_e lead to a brighter timbre—but under nonlinear conditions, increases in $F_{\max}$ can have a strong impact on timbre as well.

2.5. Output

For synthesis purposes, it is probably overkill to use a complete model of the sound path from the instrument to the listener—a crude but effective strategy, used across many physical modeling methods, is to read output velocity from a point or distribution on the surface of one of the elements, and then apply post-processing to emulate effects of sound directionality and/or room reverberation, if desired. To this end, an output $y(t)$ may be defined as

$$y = \langle E_o, u_t \rangle$$

where as before, the bracket notation indicates an L_2 inner product over the appropriate space (1D or 2D, depending on the element). The distribution E_o, in the simplest case, could be a Dirac delta function, selecting ouput velocity at a given output location.

3. FINITE DIFFERENCE SCHEMES

3.1. Bars

In 1D, a grid function u_l^n represents an approximation to a continuous function $u(x,t)$, at grid locations $x = lh$ and at times $t = nk$, for integer l and n, where h is the grid spacing, and k is the time step (and $1/k$ is the sample rate, normally chosen a priori in audio applications). When the spatial domain is the unit interval, it is convenient to choose $h = 1/N$, for some integer N, so that the index l runs from $l = 0, \ldots, N$.

Difference operators may be defined as

$$\delta_{tt} u_l^n = \frac{1}{k^2}\left(u_l^{n+1} - 2u_l^n + u_l^{n-1}\right) \quad (11a)$$

$$\delta_{t\cdot} u_l^n = \frac{1}{2k}\left(u_l^{n+1} - u_l^{n-1}\right) \quad (11b)$$

$$\delta_{t-} u_l^n = \frac{1}{k}\left(u_l^n - u_l^{n-1}\right) \quad (11c)$$

$$\delta_{xx} u_l^n = \frac{1}{h^2}\left(u_{l+1}^n - 2u_l^n + u_{l-1}^n\right) \quad (11d)$$

The first is an approximation to a second time derivative, the second and third to a first time derivative, and the fourth to a second spatial derivative.

Such operators may be employed to arrive at a scheme for a bar, beginning from the form (2):

$$\delta_{tt} u = -\kappa^2 \delta_{xx}\delta_{xx} u - 2\sigma_0 \delta_{t\cdot} u + 2\sigma_1 \delta_{t-}\delta_{xx} u + \sum_q E_q F_q \quad (12)$$

Here, $F_q = F_q^n$ is now a time series, and $E_q = E_{q,l}$ is a grid function corresponding to the continuous distribution $E_q(x)$ (obtained via sampling, or, if the distribution is very sharply peaked, other interpolation techniques [16]). This scheme is explicit in the absence of connections, and a necessary condition for stability is that

$$h \geq h_{\min} = \sqrt{2k\left(\sigma_1^2 + \sqrt{\kappa^2 + \sigma_1^2}\right)} \quad (13)$$

leading to a maximum of $N = \mathrm{floor}(1/h_{\min})$ for the number of grid points covering the unit interval. Though the scheme appears to make use of values of the grid function outside the unit interval, numerical boundary conditions corresponding to (3) may be employed to set such values in terms of values over the interior of the domain. If such conditions are properly chosen (see [16] for some choices), the above stability condition becomes sufficient (and will remain so, even under nonlinear connection conditions, provided the nonlinear connections are discretized is a special way—see Section 3.3). In a network configuration, the grid spacing can (and should) be chosen independently for each instance of a bar.

3.2. Plates

In 2D, a grid function $u_{l,m}^n$ represents an approximation to a continuous function $u(x,y,t)$, at grid locations $x = lh_x$, $y = mh_y$, for integer l, m and n, where k is, as before, the time step, and where h_x and h_y are grid spacings in the x and y directions respectively. Though these may be chosen independently, they will be assumed here, for simplicity, to be equal, i.e., $h_x = h_y = h$. (For a plate defined over a unit area rectangle of aspect ratio α, it is probably easiest to choose $h = \sqrt{\alpha}/N_x$, for some integer N_x, and then set $N_y = \mathrm{floor}(N_x/\alpha)$.)

The time difference operators given in (11) extend to 2D in an obvious way; a simple approximation to the Laplacian, as given in (5), is

$$\delta_\Delta u_{l,m}^n = \frac{1}{h^2}\left(u_{l,m+1}^n + u_{l,m-1}^n + u_{l+1,m}^n + u_{l-1,m}^n - 4u_{l,m}^n\right)$$

A scheme for (6) then follows as

$$\delta_{tt} u = -\kappa^2 \delta_\Delta \delta_\Delta u - 2\sigma_0 \delta_{t\cdot} u + 2\sigma_1 \delta_{t-}\delta_\Delta u + \sum_q E_q F_q \quad (14)$$

where as in the case of the bar, $F_q = F_q^n$ is now a time series, and where $E_q = E_{q,l,m}$ is a 2D discrete distribution.

A stability condition for the above scheme, again under appropriate boundary terminations corresponding to (7), is

$$h \geq h_{\min} = 2\sqrt{k\left(\sigma_1^2 + \sqrt{\kappa^2 + \sigma_1^2}\right)} \quad (15)$$

again leading to maximum values of the grid size (N_x, N_y).

3.3. Connections

For the connecting elements, it is useful to introduce semi-implicit methods, which have excellent stability properties—wave digital filters, in the linear case, are one instance of such a method, but there are many others. As the connection element, as defined in (8a) is lumped, it will be necessary to approximate the quantities $F(t)$ and $\eta(t)$ as time series F^n and η^n. In addition to the centered time difference operator, as defined in (11b) (and now applied not to a grid function but a time series), an averaging operator is also useful. To this end, define the operator $\mu_{t\cdot}$, as applied to a time series η as

$$\mu_{t\cdot}\eta^n = \frac{1}{2}\left(\eta^{n+1} + \eta^{n-1}\right)$$

A semi-implicit discretization of (8a) is then

$$F_c = -\omega_0^2 \mu_{t\cdot}\eta - \omega_1^4 \eta \mu_{t\cdot}\eta - 2\sigma_\times \delta_{t\cdot}\eta \quad F_c^* = -\mathcal{M}_{1/2} F_c$$

Though nonlinear, this update may be solved uniquely for the unknown value of η at time step $n+1$, in terms of previously computed values of F and η (i.e., up through time step n):

$$\eta^{n+1} = p^n F_c^n + r^n \eta^{n-1} \quad (16)$$

where

$$p^n = \frac{-2}{2\sigma_x/k + \omega_0^2 + \omega_1^4(\eta^n)^2} \quad (17a)$$

$$r^n = \frac{2\sigma_x/k - \omega_0^2 - \omega_1^4(\eta^n)^2}{2\sigma_x/k + \omega_0^2 + \omega_1^4(\eta^n)^2} \quad (17b)$$

The discrete definition of η corresponding to (9) is postponed until the next section, after matrix representations have been introduced.

The above system of difference equations, combined with updates for the individual elements, as described in the preding sections, is stable, as long as the stability conditions (13) and (15) are respected—a full proof is impossible here, but is carried out for systems of this type in [16]. In short, the system may be shown to be strictly dissipative under transient conditions, and when excitations are present, the size of the state of the system may be bounded in terms of supplied energy. What is more, as will be seen shortly, it also admits a unique solution update, which is something of a rarity for stable methods for nonlinear systems.

3.4. Matrix Representations

Looking towards implementation, it is useful to rewrite the above schemes in a vector-matrix form. For the scheme (12), one may define the column vector state $\mathbf{u}^n$ as

$$\mathbf{u}^n = [u_0^n, \ldots, u_N^n]^T$$

and for scheme (14), the 2D grid function $u_{l,m}^n$ may be "flattened" to a vector $\mathbf{u}^n$, by concatenating consecutive vertical strips as

$$\mathbf{u}^n = [u_{0,0}^n, \ldots, u_{0,N_y}^n, \ldots, u_{N_x,0}^n, \ldots, u_{N_x,N_y}^n]^T$$

Assuming, for the moment, that no couplings or excitations are present, the schemes (12) and (14), then, may be written in the same general two-step update form as

$$\mathbf{u}^{n+1} = \mathbf{B}\mathbf{u}^n + \mathbf{C}\mathbf{u}^{n-1} \quad (18)$$

Here, the matrices $\mathbf{B}$ and $\mathbf{C}$ are defined as

$$\mathbf{B} = \frac{1}{1+\sigma_0 k}\left(2\mathbf{I} - \kappa^2 k^2 \mathbf{D}^{(4)} + 2\sigma_1 k \mathbf{D}^{(2)}\right)$$

$$\mathbf{C} = -\frac{1}{1+\sigma_0 k}\left((1-\sigma_0 k)\mathbf{I} + 2\sigma_1 k \mathbf{D}^{(2)}\right)$$

where here, $\mathbf{D}^{(2)}$ and $\mathbf{D}^{(4)}$ are square matrices corresponding to the operators δ_{xx} (or δ_Δ) and $\delta_{xx}\delta_{xx}$ (or $\delta_\Delta\delta_\Delta$), with appropriate boundary conditions taken into account, and $\mathbf{I}$ is an identity matrix of the appropriate size. For a bar, the matrices $\mathbf{B}$ and $\mathbf{C}$ will be of size $(N+1)\times(N+1)$, and for the plate, of size $(N_x+1)(N_y+1)\times(N_x+1)(N_y+1)$. They are very sparse, and possess a nearly Toeplitz form (nearly block Toeplitz in the case of the plate), with perturbations due to the particular choice of boundary condition.

In preparation for the introduction of connections and excitation, it is useful to consider the case of Q such systems, of bar or plate type. Supposing that the states and corresponding matrices are $\mathbf{u}_q$, $\mathbf{B}_q$, and $\mathbf{C}_q$, for $q = 1, \ldots, Q$, then a combined update may be written as

$$\bar{\mathbf{u}}^{n+1} = \bar{\mathbf{B}}\bar{\mathbf{u}}^n + \bar{\mathbf{C}}\bar{\mathbf{u}}^{n-1}$$

where $\bar{\mathbf{u}} = [\mathbf{u}_1^T, \ldots, \mathbf{u}_Q^T]^T$, and where the block diagonal matrices $\bar{\mathbf{B}}$ and $\bar{\mathbf{C}}$ are formed as the direct sums of the individual matrices $\mathbf{B}_q$ and $\mathbf{C}_q$, $q = 1, \ldots, Q$. If the sizes of the individual vectors $\mathbf{u}_q$ are N_q, then the total size of the state $\mathbf{u}$ will be $\bar{N} = \sum_{q=1}^Q N_q$.

3.5. A Complete Network

When Q_c connections and Q_e excitations are present, the above update may be generalized as

$$\bar{\mathbf{u}}^{n+1} = \bar{\mathbf{B}}\bar{\mathbf{u}}^n + \bar{\mathbf{C}}\bar{\mathbf{u}}^{n-1} + \bar{\mathbf{J}}\mathbf{F}_c + \bar{\mathbf{K}}\mathbf{F}_e \quad (19)$$

Here, $\mathbf{F}_c = [F_{c,1}, \ldots, F_{c,Q_c}]^T$ and $\mathbf{F}_e = [F_{e,1}, \ldots, F_{e,Q_e}]^T$ are vectors representing the connection and excitations forces, respectively.

The matrix $\bar{\mathbf{J}} = [\bar{\mathbf{j}}_1 | \ldots | \bar{\mathbf{j}}_{Q_c}]$ describes the ensemble of connections, and is of size $\bar{N} \times Q_c$—there is a column $\bar{\mathbf{j}}_r$, $r = 1, \ldots, Q_c$ describing each connection. Each such column is a concatenation of Q sub-columns, as $\bar{\mathbf{j}}_r = [\mathbf{j}_{1,r}^T, \ldots, \mathbf{j}_{Q,r}^T]^T$; each such sub-column $\mathbf{j}_{q,r}$ is of size N_q, $q = 1, \ldots, Q$, and corresponds to a separate element in the network. If the rth connection associates elements $\alpha(r)$ and $\beta(r)$, then the elements of $\bar{\mathbf{J}}$ may be set as

$$\mathbf{j}_{\alpha(r),r} = \frac{k^2 \mathbf{E}_{c,(\alpha(r),r)}}{1+\sigma_{0,\alpha(r)}k} \qquad \mathbf{j}_{\beta(r),r} = -\frac{\mathcal{M}_{\alpha(r)/\beta(r)} k^2 \mathbf{E}_{c,(\beta(r),r)}}{1+\sigma_{0,\beta(r)}k}$$

and otherwise are zero. Here, $\mathbf{E}_{c,(\alpha(r),r)}$ and $\mathbf{E}_{c,(\beta(r),r)}$ are the two distributions associated with connection r and elements $\alpha(r)$ and $\beta(r)$, and $\sigma_{0,\alpha(r)}$ and $\sigma_{0,\beta(r)}$ are the two loss paramameters associated with elements $\alpha(r)$ and $\beta(r)$, respectively. Each such assignment above is none other than connection rule (8b), with additional factors appearing due to discretization.

Similarly, the matrix $\bar{\mathbf{K}} = [\bar{\mathbf{k}}_1 | \ldots | \bar{\mathbf{k}}_{Q_e}]$ describes the ensemble of excitations, and is of size $\bar{N} \times Q_e$; each such column $\bar{\mathbf{k}}_m$, $m = 1, \ldots, Q_e$ is similarly partitioned as $\bar{\mathbf{k}}_m = [\mathbf{k}_{1,m}^T, \ldots, \mathbf{k}_{Q,m}^T]^T$. If the mth excitation is associated with element $\alpha(m)$, through an excitation distribution $\mathbf{E}_{e,(\alpha(m),m)}$, then the elements of $\bar{\mathbf{K}}$ may be set as

$$\mathbf{k}_{\alpha(m),m} = \frac{k^2 \mathbf{E}_{e,(\alpha(m),m)}}{1+\sigma_{0,\alpha(m)}k}$$

and are otherwise zero.

Associated with the vector of forces $\mathbf{F}_c$ is a set of relative displacements $\boldsymbol{\eta} = [\eta_1, \ldots, \eta_{Q_c}]^T$; these will be related, from (16), at time step n, as

$$\boldsymbol{\eta}^{n+1} = \mathbf{P}^n \mathbf{F}_c^n + \underbrace{\mathbf{R}^n \boldsymbol{\eta}^{n-1}}_{\triangleq \mathbf{a}^n} \quad (20)$$

where $\mathbf{P}^n$ and $\mathbf{R}^n$ are diagonal matrices containing values of p^n and r^n, as given in (17) on the diagonal. The vector $\mathbf{a}^n$ consists of previously computed values of the state.

It remains to write $\boldsymbol{\eta}$ in terms of the state $\bar{\mathbf{u}}$; this can be done by applying a discrete version of the inner products given in (9). In order to determine η_r^n, the relative displacement associated with connection r, one may write

$$\eta_r^n = \sigma_{c,(\alpha(r),r)} \mathbf{E}_{c,(\alpha(r),r)}^T \mathbf{u}_{\alpha(r)}^n - \sigma_{c,(\beta(r),r)} \mathbf{E}_{c,(\beta(r),r)}^T \mathbf{u}_{\beta(r)}^n \quad (21)$$

where $\sigma_{c,(\alpha(r),r)}$ and $\sigma_{c,(\beta(r),r)}$ are constants equal to the grid spacing, in the case of a bar element, and the square of the grid spacing, for a plate element. In matrix form, then, one has

$$\boldsymbol{\eta}^n = \bar{\mathbf{L}}\bar{\mathbf{u}}^n \quad (22)$$

or, employing (19),

$$\boldsymbol{\eta}^{n+1} = \underbrace{\left(\bar{\mathbf{L}}\bar{\mathbf{B}}\bar{\mathbf{u}}^n + \bar{\mathbf{L}}\bar{\mathbf{C}}\bar{\mathbf{u}}^{n-1} + \bar{\mathbf{L}}\bar{\mathbf{K}}\mathbf{F}_e^n\right)}_{\triangleq \mathbf{b}^n} + \bar{\mathbf{L}}\bar{\mathbf{J}}\mathbf{F}_c^n \quad (23)$$

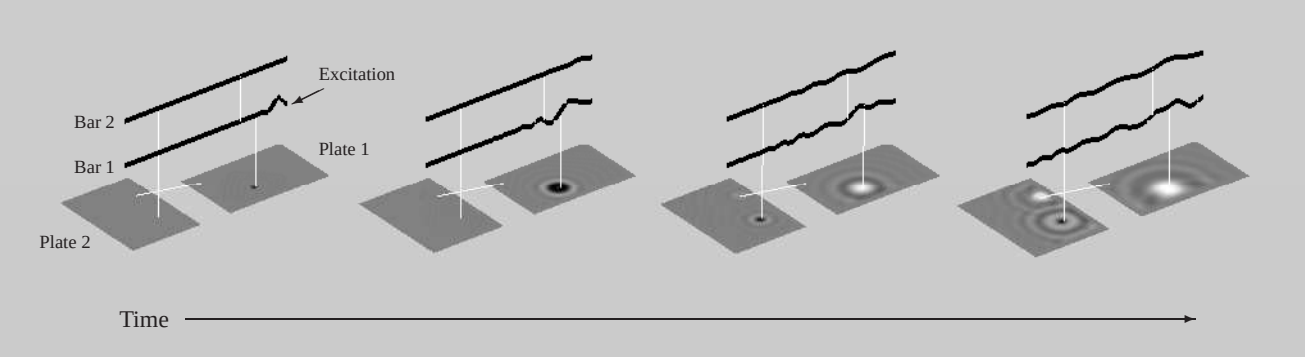

Figure 2: *Snapshots of the time evolution of a network composed of two bars and two plates, all under clamped boundary conditions. Energy supplied by a strike applied to bar 1 is transmitted to plate 1 and bar 2, then subsequently to plate 2 via both bar 2 and plate 1.*

where $\mathbf{b}^n$ consists of previously computed values of the state, as well as known values of the excitations. Finally, (20) and (23) may be combined to give a unique solution for $\mathbf{F}_c$:

$$\left(\bar{\mathbf{L}}\bar{\mathbf{J}} - \mathbf{P}\right)\mathbf{F_c} = \mathbf{a}^n - \mathbf{b}^n \tag{24}$$

Despite the rather complicated formalism here, this linear system to be solved will be of the order of the number of connections in the network, and thus, in most cases, relatively small—furthermore, if the various distributions that describe the connections are non-overlapping (this is often the case for percussive excitations, which are highly localized), the system to be solved is diagonal. Once the connection forces $\mathbf{F}_c$ are known, scheme (19) may then be updated explicitly.

Referring to Section 2.5, Q_o-channel output $\mathbf{y}^n$ may be derived from the state $\bar{\mathbf{u}}^n$ in a feedforward step, as

$$\mathbf{y}^n = \mathbf{S}\delta_{t-}\bar{\mathbf{u}}^n$$

where here, $\mathbf{y}^n$ is a $Q_o \times 1$ vector, and where $\mathbf{S}$ is a $Q_o \times \bar{N}$ matrices, the rows of which consist of discrete output distributions $\mathbf{E}_o$, generally peaked about some set of output locations, and δ_{t-} is a first time difference, as defined in (11c). Note that in a time domain fomulation, it is quite straightforward to allow the output locations to be time-varying—such is not the case in a modal implementation.

4. SIMULATION RESULTS AND SOUND SYNTHESIS EXAMPLES

This structure has been implemented in the Matlab prototyping language. Memory requirements, for a bar element with stiffness parameter κ, scale with $\sqrt{f_s/\kappa}$, and for a plate, with f_s/κ units of storage, where f_s is the sample rate, and are thus not extreme, given that κ usually lies in the range between 5 and 200 for musical systems. The operation count/second scales with the memory times the sample rate f_s, due to the sparseness of the finite difference update. An illustration of simulation results for a simple system is as shown in Figure 2—sound examples, drawn from much more complex configurations involving 20–50 individual components, and as many connections, are provided on the author's website, at `http://ccrma.stanford.edu/~bilbao/soundex/bpnet/` Given that the space of possible timbres becomes very large, even for a modest number of elements and connections, it is useful to explore some of the most basic features with reference to simple networks consisting of two elements and a single connection.

4.1. A Bar/Bar Connection

Considering first the case of two bars. Supposing first that the bars are lossless, and that the connection consists of a single linear spring, then plots of output spectra are informative. The modal frequencies of the combination, and especially the lowest such frequencies, which serve as strong pitch cues, depend in a complicated way on the stiffness parameter, and also on the location of the connection, as well as the mass ratio between the bars—see Figure 3, illustrating some such variations. In general, such a connection can lead to highly dissonant sound output, far beyond that inherent to individual bars.

Further variations of this basic structure involve the linear damper, and nonlinear spring mechanism—spectrograms of sound output are shown in Figure 4. The linear damper leads, obviously, to to a shorter over-all decay time, but there are pronounced variations in the rates of decay of various components, as in Figure 4(a). When a nonlinear spring is employed, in conjunction with a damper, there can be a dramatic noise-like burst in the attack portion of a strike, accompanied by a downward pitch glide, as illustrated in Figure 4(b); pitch glides are typical perceptual features of plucked string and percussion instruments, under high amplitude excitation.

4.2. A Bar/Plate Connection

An interesting configuration of a bar/plate connection is one for which the bar behaves as the primary vibrating element, and the plate as an auxiliary resonator—such a configuration is similar to a string/soundboard connection, or a plate reverberation system, if the stiffness parameter κ of the plate is chosen very small (on the order approximately $\kappa = 2$ or lower).

One set of output spectra is as shown in Figure 5, for different choices of the bar/plate mass ratio, with output drawn from the bar—notice that such results are considerably more general than those obtained using commuted synthesis techniques [23], in that the coloration of the resulting timbre (i.e., the positions and strengths of the various partials in the output) will be dependent on not just this mass ratio, but also the location and parameters defining the connection itself. It is, of course, possible for the bar and plate to switch roles, with the plate behaving as the primary vibrating element, and the bar as a resonator.

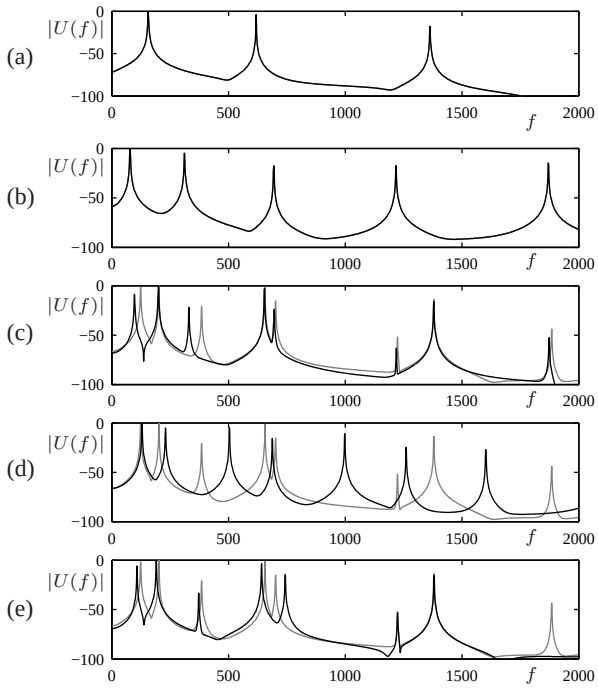

Figure 3: *Output magnitude spectra $|U(f)|$, in dB, as a function of frequency f in Hz, for a combination of two lossless bars, of stiffness parameters $\kappa = 100$ and $\kappa = 50$, under pivoting end conditions, connected with a linear spring. In all cases, input is applied and output read at locations 0.3 and 0.7 of the way from the left end of the bar. In (a), and (b) output spectra for uncoupled bars. In the following panels are shown, in grey the output spectrum from the first bar, under a reference connection with $\omega = 1000$, and at location $x = 0.8$ (first bar) and $x = 0.3$ (second bar), and where the mass ratio of the second bar to the first is 1. In (c), in black, the output spectrum when the mass ratio is 4, in (d), in black, the output spectrum when $\omega_0 = 4000$, and in (e), in black, the output spectrum when the position of coupling to the second bar is changed to $x = 0.8$.*

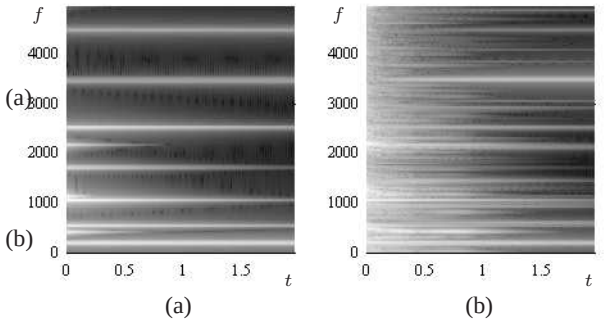

Figure 4: *Spectrograms of sound output, as a function of time t, in seconds, and frequency f in Hz, for a conection of two bars, of parameters as described in the caption to Figure 3, under (a) a linear damper connection, and (b) a nonlinear spring connection, accompanied by a damper.*

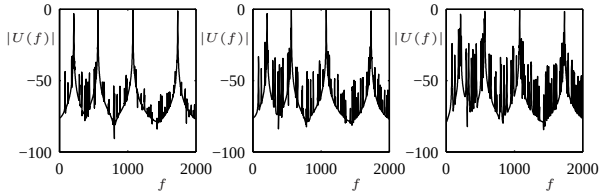

Figure 5: *Output magnitude spectra $|U(f)|$, in dB, as a function of frequency f in Hz, for output of a combination of a bar, with $\kappa = 50$, and a plate, with $\kappa = 10$, and aspect ratio $\alpha = 1.3$; both are under clamped boundary conditions. There is a connection, via a linear spring of stiffness parameter $\omega_0 = 1000$, connected to the bar at position $x = 0.8$, and to the plate at position $x = 0.4$, $y = 0.3$. Variations in the output spectrum are shown, for different choices of the plate/bar mass ratio: (a) 10000, (b) 1000 and (c) 100, where output is drawn from the bar at $x = 0.9$.*

4.3. A Plate/Plate Connection

The modal frequencies of a plate are highly inharmonic though the modal density is uniform, and when a nonlinearity is present in a connection between two such plates, new perceptual phenomena, beyond pitch glides are possible, and in particular, the generation of noise-like outputs which resemble cymbal crashes under high amplitude excitations. See Figure 6.

5. CONCLUSION

The model presented here is made up of abstract distributed components, and a set of nonlinear connections—the main point here is that an appeal to elaborate network theory constructions, and the introduction of wave variables, as is seen in scattering-based approaches to modular sound synthesis is not really necessary—the sum total of network theory principles necessary to manage possibly many inter-element connections is summarized in the equations (8) and (9); there are no data flow or computability issues, as all nonlinearities are handled simultaneously in a single (small) linear system solution, as given in (24). Precomputation consists mainly of forming the updating arrays, which, while not trivial, is not intensive in terms of memory or operation counts, unlike the procedure necessary for determining modal data. Stability follows definitively for the network as presented here—this property is in part due to the special form of the nonlinearities (cubic) which appear here, and is no longer strictly true when other types of nonlinearity are employed—among the forms that would be of interest are one-sided forms, allowing for rattling and collisions among elements.

This model may be extended to incorporate elements of string and membrane type very easily; this will affect the internal structure of the matrices $\bar{\mathbf{B}}$ and $\bar{\mathbf{C}}$ only, and not the connection machinery. Higher computational costs will result, however, for these systems—this is a fundamental concern for such systems across all physical modeling methodologies, except for the case of strings, where waveguide solutions are more efficient. The finite difference model, unlike other types of synthesis strategies, may be extended to the case of fully nonlinear bar and plate vibration, though extra work at the level of algorithm design is necessary in order to maintain a stability property [24, 25].

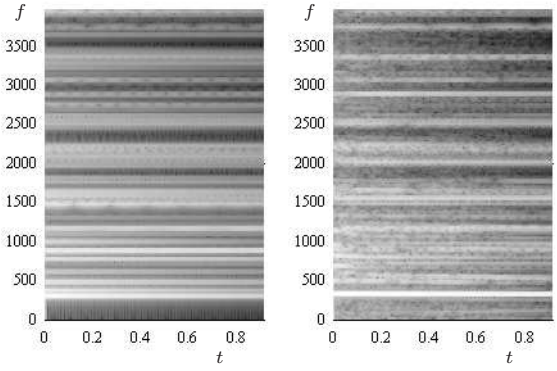

Figure 6: *Output spectrograms, as a function of frequency f, in Hz, and time t in seconds, for output from a connection between two lossless plates, of stiffness parameters $\kappa = 50$ and $\kappa = 40$, and aspect ratios $\alpha = 1.3$ and 1.4, under clamped boundary conditions. The connection is of the form of a damper, combined with a nonlinear spring, attached at the plate centers. Responses of the second plate to a strike on the first are shown for (a) low-amplitude excitation, and (b) high-amplitude excitation.*

6. REFERENCES

[1] C. Cadoz, "Synthèse sonore par simulation de mécanismes vibratoires," 1979, Thèse de Docteur Ingénieur, I.N.P.G. Grenoble, France.

[2] C. Cadoz, A. Luciani, and J.-L. Florens, "Responsive input devices and sound synthesis by simulation of instrumental mechanisms," *Computer Music Journal*, vol. 8, no. 3, pp. 60–73, 1983.

[3] C. Cadoz, A. Luciani, and J.-L. Florens, "Cordis-anima: A modeling and simulation system for sound and image synthesis," *Computer Music Journal*, vol. 17, no. 1, pp. 19–29, 1993.

[4] J.-L. Florens and C. Cadoz, "The physical model: Modeling and simulating the instrument universe," in *Representations of Musical Signals*, G. DePoli, A. Picialli, and C. Roads, Eds., pp. 227–268. MIT Press, Cambridge, Massachusetts, 1991.

[5] D. Morrison and J.-M. Adrien, "Mosaic: A framework for modal synthesis," *Computer Music Journal*, vol. 17, no. 1, pp. 45–56, 1993.

[6] J.-M. Adrien, "The missing link: Modal synthesis," in *Representations of Musical Signals*, G. DePoli, A. Picialli, and C. Roads, Eds., pp. 269–297. MIT Press, Cambridge, Massachusetts, 1991.

[7] L. Trautmann and R. Rabenstein, *Digital Sound Synthesis by Physical Modeling Using the Functional Transformation Method*, Kluwer Academic/Plenum Publishers, New York, New York, 2003.

[8] R. Rabenstein, S. Petrausch, A. Sarti, G. De Sanctis, C. Erkut, and M. Karjalainen, "Block-based physical modeling for digital sound synthesis," *IEEE Signal Processing Magazine*, vol. 24, no. 2, pp. 42–54, 2007.

[9] M. Karjalainen and C. Erkut, "Digital waveguides vs. finite difference schemes: Equivalence and mixed modeling," *EURASIP Journal on Applied Signal Processing*, vol. 7, pp. 978–989, 2004.

[10] V. Välimäki, J. Pakarinen, C. Erkut, and M. Karjalainen, "Discrete time modeling of musical instruments," *Reports on Progress in Physics*, vol. 69, pp. 1–78, 2006.

[11] K. van den Doel, "Modal synthesis for vibrating objects," in *Audio Anecdotes III*, K. Greenebaum, Ed. A. K. Peters, Natick, Massachusetts, 2007.

[12] T. Hélie and D. Roze, "Sound synthesis of a nonlinear string using Volterra series," *Journal of Sound and Vibration*, vol. 314, no. 1–2, pp. 275–306, 2008.

[13] S. Petrausch and R. Rabenstein, "Tension modulated nonlinear 2D models for digital sound synthesis with the functional transformation method," in *Proceedings of EUSIPCO-05, Thirteenth European Signal Processing Conference*, Antalya, Turkey, September 2005.

[14] F. Pedersini, A. Sarti, S. Tubaro, and R. Zattoni, "Towards the automatic synthesis of nonlinear wave digital models for musical acoustics," in *Proceedings of EUSIPCO-98, Ninth European Signal Processing Conference*, Rhodes, Greece, 1998, vol. 4, pp. 2361–2364.

[15] G. DeSanctis, A. Sarti, and S. Tubaro, "Automatic synthesis strategies for object-based dynamical physical models in musical acoustics," in *Proceedings of the COST-G6 Digital Audio Effects Conference*, London, UK, September 2003, pp. 219–224.

[16] S. Bilbao, *Numerical Sound Synthesis: Finite Difference Schemes and Simulation in Musical Acoustics*, John Wiley and Sons, Chichester, UK, 2009, in press.

[17] N. Fletcher and T. Rossing, *The Physics of Musical Instruments*, Springer-Verlag, New York, New York, 1991.

[18] B. Guo and W. Guo, "Adaptive stabilization for a Kirchhoff-type nonlinear beam under boundary output feedback control," *Nonlinear Analysis*, vol. 66, pp. 427–441, 2007.

[19] V. Doutaut, D. Matignon, and A. Chaigne, "Numerical simulations of xylophones. II. Time domain modeling of the resonator and of the radiated sound pressure," *Journal of the Acoustical Society of America*, vol. 104, no. 3, pp. 1633–1647, 1998.

[20] P. Morse and U. Ingard, *Theoretical Acoustics*, Princeton University Press, Princeton, New Jersey, 1968.

[21] K. Graff, *Wave Motion in Elastic Solids*, Dover, New York, New York, 1975.

[22] L. Rhaouti, A. Chaigne, and P. Joly, "Time-domain modeling and numerical simulation of a kettledrum," *Journal of the Acoustical Society of America*, vol. 105, no. 6, pp. 3545–3562, 1999.

[23] J. O. Smith III and S. van Duyne, "Commuted piano synthesis," in *Proceedings of the International Computer Music Conference*, Banff, Canada, 1995, pp. 319–326.

[24] S. Bilbao, "A family of conservative finite difference schemes for the dynamical von Karman plate equations," *Numerical Methods for Partial Differential Equations*, vol. 24, no. 1, pp. 193–216, 2008.

[25] S. Bilbao, "Conservative numerical methods for nonlinear strings," *Journal of the Acoustical Society of America*, vol. 118, no. 5, pp. 3316–3327, 2005.